

## Experimental Application of Strain Gauge Rosette and Determination of Principal Strains Using Mohr Circle

Orhorhoro EK<sup>1\*</sup>, Ikpe AE<sup>2</sup>, Olorunleke A<sup>1</sup>

<sup>1</sup>Department of Mechanical Engineering, College of Engineering, Igbinedion University, Okada, Nigeria  
<sup>2</sup>Room 142, Department of Mechanical Engineering, University of Benin, Nigeria

\*Corresponding author: Orhorhoro EK

| Received: 13.05.2019 | Accepted: 20.05.2019 | Published: 30.05.2019

DOI: [10.36347/sjet.2019.v07i05.006](https://doi.org/10.36347/sjet.2019.v07i05.006)

### Abstract

### Original Research Article

The objective of the experiment was to understand the practical application of strain gauge rosette and to determine principal strains and their direction using Mohr circle. Elastic constants of the specimen were evaluated using the values obtained from the experiment. The constants gotten from the experiment were compared with the standard elastic constants for steel. The comparison showed that the elastic constants evaluated from the experiment were very close to the standard ones. The small difference in their values can be attributed to experimental errors which cannot be completely avoided.

**Keywords:** Strain gauge rosette, principal strains, Mohr circle, elastic constant, experimental errors.

**Copyright © 2019:** This is an open-access article distributed under the terms of the Creative Commons Attribution license which permits unrestricted use, distribution, and reproduction in any medium for non-commercial use (NonCommercial, or CC-BY-NC) provided the original author and source are credited.

## INTRODUCTION

A strain gauge rosette is an arrangement of two or more closely positioned strain gauge grids, separately oriented to measure the normal strains along different directions in the underlying surface of the test part [1]. There are many types of strain gauges, but the common ones are the rectangular and delta types. In the rectangular type, the second and the third grids are 0°, 45° and 90° apart from the first grid while for the delta type, the three gages placed at the 0°, 60°, and 120° positions [2]. Strain gauge rosettes, like other strain gauges employ the change in electrical resistance of a wire due to change in length in measuring strain. The resistance of an electrical conductor is directly proportional to the length and inversely to the cross sectional [4] as shown in the equation below:

$$R = \frac{\rho L}{A} \quad (1)$$

where, R is electrical resistance,  $\rho$  is Specific resistance of material, L is the length, A is cross sectional area

The working of the strain gauge rosette is based on equation (1). When the strain gauge rosette is firmly attached to the surface of a material on which strain is to be measured, the thin wire inside in each of the grid elongates or contracts with the material when force is applied to the material. Due to the change in length and/ or cross-sectional area of the wires inside

the strain gauge rosette, their resistance also changes proportionally. This change of resistance is measured using a strain gauge indicator. The strain is displayed by properly converting the change in resistance to strain [5]. One way of straining a material is by tensile test. Tensile test is one of the basic mechanical tests performed on a material. A test piece is firmly gripped to a tensile test machine. By pulling the test piece, the force required to elongate the test piece can be calculated. This test is important as the force require to break a material can be calculated. The test is also used to determine the properties of the material like tensile strength, strain, Young's Modulus and Poisson ratio which are used to predict the behaviour of the material under loading. In this research work, the principal strains of the test piece, the properties of the material such as Young's Modulus and Poisson ratio were determined. To perform this experiment, a strain gauge rosette was firmly attached to a steel beam undergoing tensile test.

## RESEARCH METHODOLOGY

### Theoretical Model

To completely measure the full state of strain on the surface of the part with xy-axis system, it is essential to measure the extensional strains,  $\epsilon_x$  and  $\epsilon_y$  as well as the shear strain  $\gamma_{xy}$ . If the x and y axes are specified, it would be possible to mount two strain gauges in the x and y directions to measure the strains in these directions. The challenge is that there is no

direct way to measure the shear strain,  $\gamma_{xy}$ . However, since the state of an existing two-dimensional surface can be expressed in terms of three cartesian strains  $\epsilon_{xx}$ ,  $\epsilon_{yy}$  and  $\gamma_{xy}$ , a completely defined strain state of 2D surface can be used to compute strains with respect to any other coordinate system. Hence, if it is possible to measure three independent values of strain at a point on the surface, then these three independent values can be

gotten. The simplest way to achieve this is to place three strain gauges together in a rosette format with each gauge placed at a different angle and all the gauges placed close to each other to approximate a measurement at a point. Three strain gauges placed along axes A, B, and C, and  $45^\circ$  apart from each other to form a rectangular strain gauge rosette as shown in Fig.1.

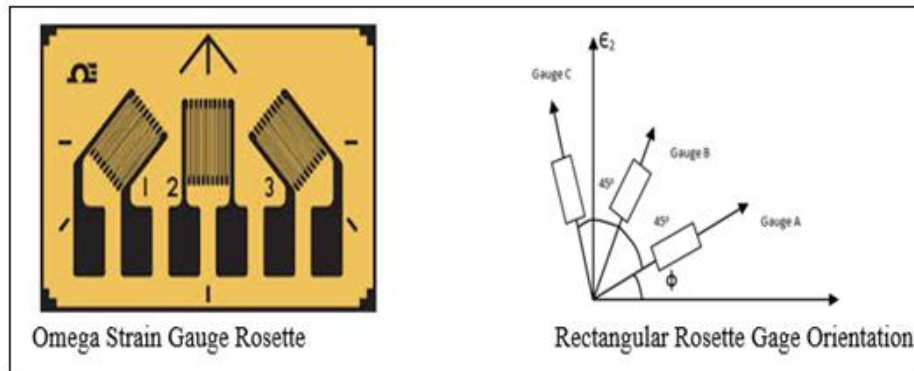


**Fig-1: Rectangular Strain Gauge Rosette**

Given 3 independent strains values from the strain gauges rosette, it is possible to calculate the principal strains and their orientation with respect to the rosette gauge. For the rectangular strain gauge in Fig.1, the strain transformation equation is given by;

$$\epsilon_A = [(\epsilon_1 + \epsilon_2)/2] + (\epsilon_1 - \epsilon_2)/2 \cos 2\phi \quad (2)$$

$$\epsilon_B = [(\epsilon_1 + \epsilon_2)/2] + (\epsilon_1 - \epsilon_2)/2 \cos 2(\phi + 45^\circ) \quad (3)$$

$$\epsilon_C = [(\epsilon_1 + \epsilon_2)/2] + (\epsilon_1 - \epsilon_2)/2 \cos 2(\phi + 90^\circ) \quad (4)$$

Solving the three equations simultaneously, the principal axis and their direction are given by

$$\epsilon_{1,2} = [(\epsilon_A + \epsilon_C)/2] \pm (1/\sqrt{2}) * \sqrt{(\epsilon_A - \epsilon_B)^2 + (\epsilon_B - \epsilon_C)^2} \quad (5)$$

$$\Phi = 0.5 \tan^{-1}((\epsilon_A - 2\epsilon_B + \epsilon_C)/(\epsilon_A - \epsilon_C)) \quad (6)$$

The maximum shear strain is given by

$$\gamma_{\max} = \epsilon_1 - \epsilon_2 \quad (7)$$

One way of determining the principal axes on which the strain acts is by constructing Mohr circle. If it assumes that the rosette oriented such that gauge A is along the x axis and gauge C is along the y axis, equation 2 to 4 is then be reduced to;

$$\epsilon_x = \epsilon_A \quad (8)$$

$$\epsilon_y = \epsilon_C \quad (9)$$

$$\gamma_{xy} = 2\epsilon_B - \epsilon_A - \epsilon_C \quad (10)$$

The values of  $\epsilon_x$ ,  $\epsilon_y$ ,  $\gamma_{xy}$  were used to construct the Mohr Circle.

#### Preparation of Test Samples

A steel beam of dimensions 165 mm by 24 mm by 6 mm was used for the experiment. To ensure that the strain gauge is adequately bonded to the surface of the beam, the surface on which the strain gauge is to be attached is properly prepared (Fig. 2). The surface preparation processes employed were degreasing, abrading, conditioning and neutralizing. Degreasing was done by using GC-6 Isopropyl Alcohol and gauze sponge to clean the surface of the beam. This was to remove oil, grease and other contaminants from the surface of the metal. Next, rough abrasive paper was used to remove any scales and oxides. The surface was then wetted with mild acidic solution and then abraded again using a smooth abrasive paper. This time, attention was paid to area of about 90mm from one end of the beam as the strain gauge rosette will be bonded there.

The application of mild acidic solution was to enhance the cleaning process. After abrading, the surface is again cleaned with gauze sponge and alcohol. Gauze sponge was used to dry the surface, starting from the inside of the beam to the outside to avoid contaminating the clean surface. A basic solution (M-pep neutralizer 5A) was then applied to neutralize the surface after which the surface was dried with gauze sponge. The rosette strain gauge was carefully and firmly applied at an angle to the horizontal axis on the clean surface using the M-bond adhesive provided. The next step was to solder wire leads onto the nine terminals of the strain gauge rosette. This was carefully done so as not to damage the strain gauge rosette.

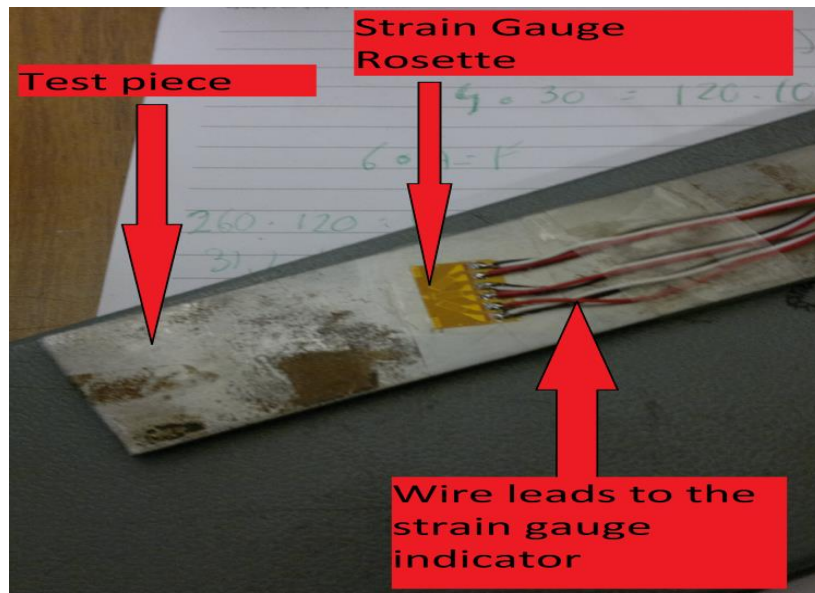


**Fig-2: Strain Gauge Rosette Bonded to the Test Piece**

Having successfully installed the rectangular strain rosette on the aluminium beam, the specimen was clamped vertically from each end of the beam on Instron tensile test machine where lead wires soldered on each of the three strain gages were connected to the input terminals (channels) of P3 Strain Indicator and Recorder illustrated in Fig. 3. The beam was firmly gripped on the INSTRON Tensile test machine 25 mm from each end of the beam. The nine leads of the strain gauge rosette were attached to the 3 channels of the gauge meter. Adequate attention was paid so as not to attach the leads of each strain gauge in a wrong

channel. Once this was done, the readings at the INSTRON display and the gauge meter were reset to zero to ensure the equipment does not display wrong data. A transparent glass shield was used to shield off the INSTRON machine to prevent the specimen from hitting anyone should it accidentally go off the machine during the test. The machine was now switched on and the specimen gradually loaded. The INSTRON machine was paused at every 13 seconds and the force, extension and Strain readings taken. The test was done three times and three sets of data obtained.

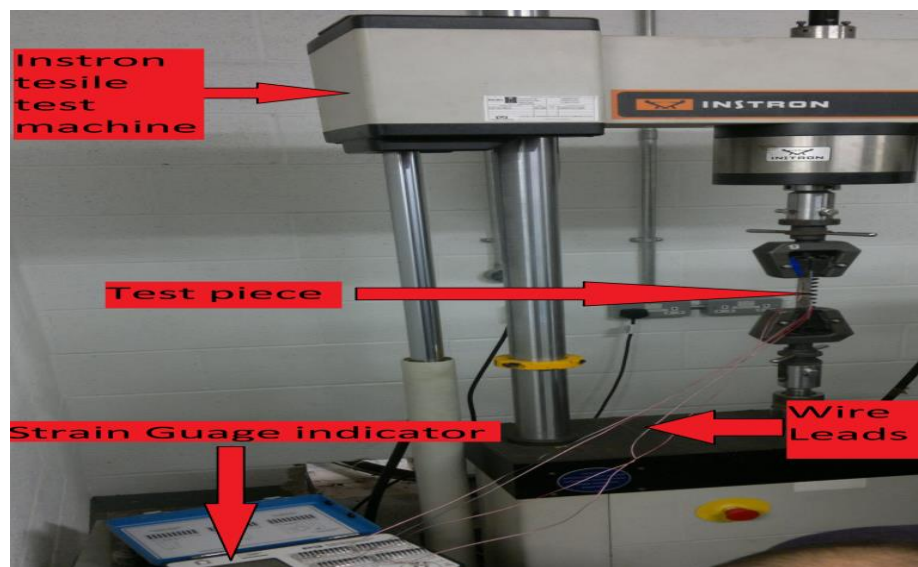


**Fig-3: Experimental Set-up Demonstrating Specimen mounted on the Instron Tensile Test Machine**

## RESULTS AND DISCUSSION

Table 1 shows the strain readings obtained from the experiment. Table 2 shows the results obtained from the plotted of Mohr Circle Graphs, and the stress

values are shown in Table 3. Table 4 shows the force, stress and young modulus values while Table 5 shows the values obtained from theoretical calculations using Equation 5, 6 and 7.

**Table-1: Strain Readings obtained from the Experiment**

Load Case 1				
S/N	Load (N)	Strain( $\mu$ ) Channel A $\epsilon_A$	Strain( $\mu$ ) Channel B $\epsilon_B$	Strain( $\mu$ ) Channel C $\epsilon_C$
Test 1	1962	-17	18	49
Test 2	1975	-14	15	37
Test 3	1969	-14	15	35
Mean	1969	-15	16	40
Standard Deviation	7	2	2	8
Standard Error	4	1	1	4
Load Case 2				
S/N	Load (N)	Strain( $\mu$ ) Channel A $\epsilon_A$	Strain( $\mu$ ) Channel B $\epsilon_B$	Strain( $\mu$ ) Channel C $\epsilon_C$
Test 1	3968	-36	45	109
Test 2	3950	-32	37	92
Test 3	3934	-32	38	91
Mean	3951	-33	40	97
Standard Deviation	17	2	4	10
Standard Error	10	1	3	6
Load Case 3				
S/N	Load (N)	Strain( $\mu$ ) Channel A $\epsilon_A$	Strain( $\mu$ ) Channel B $\epsilon_B$	Strain( $\mu$ ) Channel C $\epsilon_C$
Test 1	5771	-53	73	167
Test 2	5870	-51	66	154
Test 3	5901	-51	67	153
Mean	5847	-52	69	158
Standard Deviation	68	1	4	8
Standard Error	39	1	2	5
Load Case 4				
S/N	Load (N)	Strain( $\mu$ ) Channel A $\epsilon_A$	Strain( $\mu$ ) Channel B $\epsilon_B$	Strain( $\mu$ ) Channel C $\epsilon_C$
Test 1	7638	-70	100	224
Test 2	7866	-69	94	213
Test 3	7832	-69	96	213
Mean	7779	-69	97	217
Standard Deviation	123	1	3	6
Standard Error	71	0	2	4
Load Case 5				
S/N	Load (N)	Strain( $\mu$ ) Channel A $\epsilon_A$	Strain( $\mu$ ) Channel B $\epsilon_B$	Strain( $\mu$ ) Channel C $\epsilon_C$
Test 1	9451	-88	127	279
Test 2	9688	-86	121	270
Test 3	9719	-87	122	271
Mean	9619	-87	123	273
Standard Deviation	147	1	3	5
Standard Error	85	1	2	3

**Table-2: Results from the plotted Mohr Circle Graphs**

$\epsilon_x = \epsilon_A$							
$\epsilon_y = \epsilon_C$							
$\gamma_{xy} = 2\epsilon_B - \epsilon_A - \epsilon_C$							
	$\epsilon_x$ ( $\mu$ )	$\epsilon_y$ ( $\mu$ )	$\gamma_{xy}/2$ ( $\mu$ )	Maximum Principal Strain $\epsilon_1$ ( $\mu$ )	Minimum Principal Strain $\epsilon_2$ ( $\mu$ )	Maximum Shear Strain $\gamma_{max}$ ( $\mu$ )	Principal Angle of rotation $\phi$ ( $^\circ$ )
Load Case 1	-15	40	4	41	-15	55	4
Load Case 2	-33	97	8	98	-33	130	4
Load Case 3	-52	158	16	160	-56	224	4.5
Load Case 4	-69	217	23	220	-72	288	4.5
Load Case 5	-87	273	30	275	-90	367	4.5

**Table-3: Stress Values**

Thickness $t$ (m) = 0.006	
Width $b$ (m) = 0.024	
Unfixed Length $h$ (m) = 0.165	
Cross sectional Area = 0.000144	
Stress = Force/Cross sectional Area	
Load (N)	Stress (N/m)
1969	13673611.11
3951	27437500
5847	40604166.67
7779	54020833.33
9619	66798611.11

**Table-4: Force, Stress and Young Modulus Values**

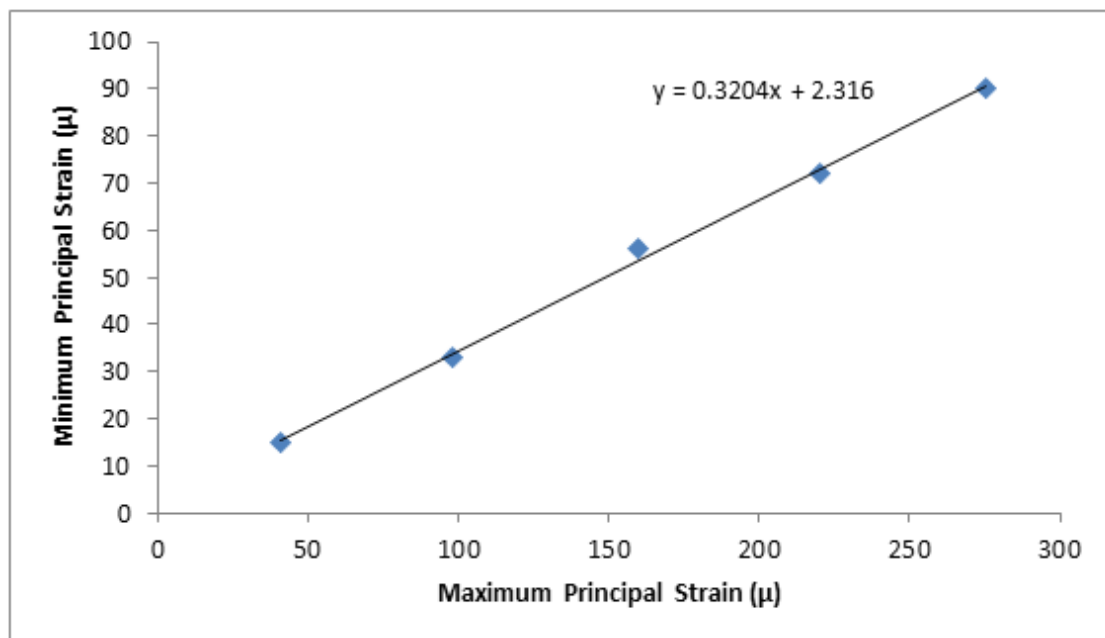
	Force (N)	Stress (N)	Strain ( $\mu$ )	Young's Modulus
Load Case 1	1969	13673611	0.000041	3.33503E+11
Load Case 2	3951	27437500	0.000098	2.79974E+11
Load Case 3	5847	40604167	0.00016	2.53776E+11
Load Case 4	7779	54020833	0.00022	2.45549E+11
Load Case 5	9619	66798611	0.000275	2.42904E+11

**Table-5: Values obtained from theoretical Calculations**

	$\epsilon_A$ ( $\mu$ )	$\epsilon_B$ ( $\mu$ )	$\epsilon_C$ ( $\mu$ )	Maximum Principal Strain $\epsilon_1$ ( $\mu$ )	Minimum Principal Strain $\epsilon_2$ ( $\mu$ )	Maximum Shear Strain $\gamma_{max}$ ( $\mu$ )	Principal Angle of rotation $\phi$ ( $^\circ$ )
Load Case 1	-15	16	40	40	-15	55	3.6
Load Case 2	-33	40	97	98	-33	131	3.5
Load Case 3	-52	69	158	159	-53	212	4.3
Load Case 4	-69	97	217	219	-71	290	4.6
Load Case 5	-87	123	273	275	-89	364	4.5

Tables 1 and 2 show the values of principal strains and their direction obtained using the Mohr circle method and theoretical calculations respectively. The values of the maximum and minimum principal strains gotten from the Mohr circle method are very close to ones obtained using theoretical calculations. Also, the principal angles differ by small margin. Fig. 4 and 5 show the graph of minimum principal strain  $\epsilon_2$  against the maximum principal strain  $\epsilon_1$  from the Mohr circles and theoretical calculations respectively. From the equation of the graphs, the slope of each graph can be determined. These slopes represent the Poisson ratio. Fig. 4 (values obtained from Mohr circle) gives a

Poisson ratio of 0.320 while Fig.5 (values obtained from theoretical calculation) gives a Poisson ratio of 0.314. When the values from the experimental is compared with the standard Poisson ratio of Steel (0.30), it was observed that the value obtained from the experiment (Fig.4) differed from the standard value by 6%. This difference can be attributed to errors which may be due to the test material not being of regular shape (for example due to dents on the surface of the specimen) and due to previous handling and use of the test piece. However, the errors were minor as the result obtained did not differ much from the standard value.

**Fig-4: Graph of Minimum Strain against Maximum Strain (From experiment)**

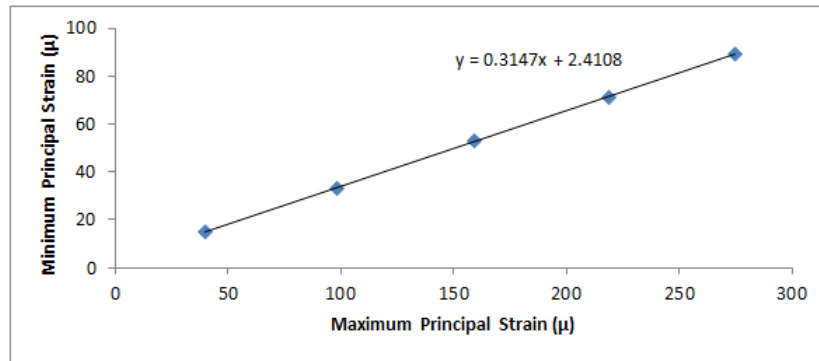


**Fig-5: Minimum Strain against Maximum Strain (Theoretical Calculation)**

Fig. 6 shows the graph of stress against the extensional strain (maximum principal strain). The slope of the graph represents the value of Young’s Modulus of the material. A slope value of  $2 \times 10^{11} \text{N/m}^2$

was obtained. This matches the standard Young’s Modulus of steel which is  $200 \times 10^9 \text{N/m}^2$ . Due to large stress values and small strain values, approximations may have made the numbers to be the same.

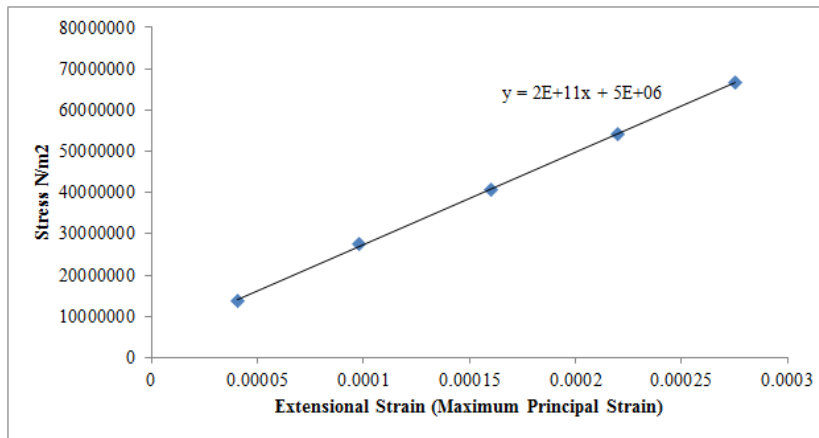


**Fig-6: Graph of Stress vs Strain (From experiments)**

When the graph of Young’s Modulus obtained from individual load case is plotted against load, a curve was obtained (Fig.7) instead of the expected horizontal line at  $200 \times 10^9 \text{N/m}^2$  as shown by Fig.8. This may have occurred due to the failure of the bonding of the strain gauge rosette to the test piece. It can be explained that the strain gauge rosette was no longer bonded by the adhesive at its centre. This made the

strain gauge rosette not to extend proportionally with the test piece during initial loading. But as loading continued up to point C on Fig. 7, the strain gauge rosette was stretched enough to start producing strains which is proportional to the force applied. From that point, the value of Young’s Modulus became fairly constant as shown from points C to D on the graph.

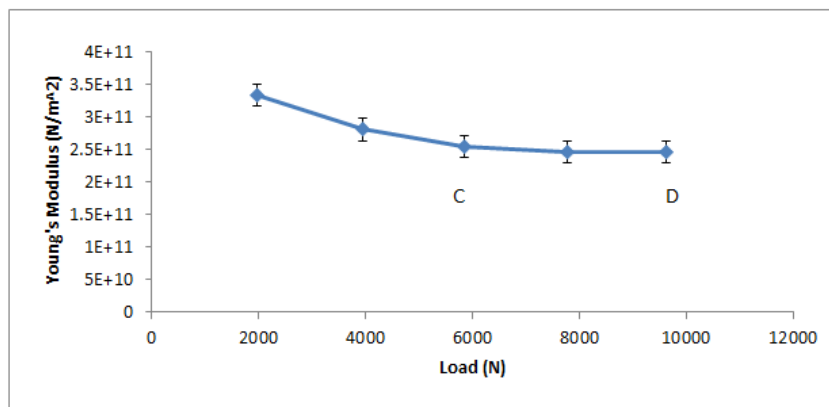


**Fig-7: Graph of Young’s Modulus against Load (Experimental Values)**

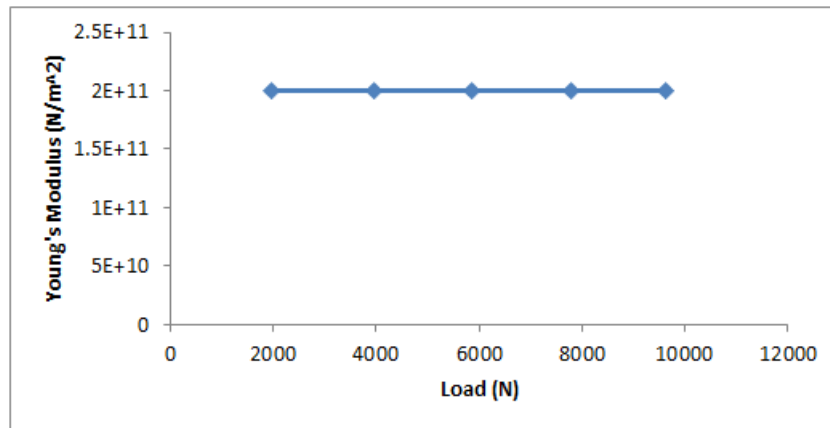


**Fig-8: Graph of Young's Modulus against Load (using standard Young's Modulus value)**

### **Possible Sources of Error**

#### **Error in Reading Variation**

While the load was added, readings on the multi-meter varied slightly as the load swung to and fro within the anchorage point of the hanger and thus, giving error in the values recorded.

#### **Electric Noise and Interference**

This was produced by the random motions of free electrons in the conductor which are in thermal equilibrium with the molecules, and its power is proportional to the absolute gauge temperature.

#### **Bridge Non-Linearity**

This was an error that produced unbalance resistance changes in the bridge arm. When the changes occurred, the voltage output of the bridge was not proportional to the resistance change, and thus the output became non-linear with the strain, therefore causing error to the strain gauge indication.

#### **Error due to the Strain Gauge Fabrication**

While conducting the experiment, it was observed that the soldered point of the strain gauge to the cantilever beam was not too strong. This might have been due to the soldering techniques, which affected the experiment exercise due to the pulling out of the loosed soldered wire.

### **CONCLUSION**

The experiment was aimed at gaining a practical understanding of Strain gauge rosette and how to use Mohr circles. Values of Young's Modulus and Poisson's ratio of steel were obtained using the values gotten from the experiment. These results were compared with standard elastic constants for steel and those obtained from theoretical calculations. The results obtained experimentally were very close to the standard values.

### **REFERENCES**

1. Dally JW, Sanford RJ. Strain gage methods for measuring the opening-mode stress intensity factor. *Exp. Mech.* 1987;27(4):381-8.
2. Khanna SK, Shukla A. On the use of strain gages in dynamic fracture mechanics. *Engineering Fracture Mechanics.* 1995 Aug 1;51(6):933-48.
3. Kuang JH, Chen LS. A single strain gage method for KI measurement. *Engineering Fracture Mechanics.* 1995 Jul 1;51(5):871-8.
4. Sarangi H, Murthy KS, Chakraborty D. Experimental verification of optimal strain gage locations for the accurate determination of mode I stress intensity factors. *Engineering Fracture Mechanics.* 2013 Sep 1;110:189-200.
5. Zanganeh M, Tomlinson RA, Yates JR. T-stress determination using thermoelastic stress analysis. *The Journal of Strain Analysis for Engineering Design.* 2008 Jun 1;43(6):529-37.